Heterogeneous Track-to-Track Fusion

Ting Yuan, Yaakov Bar-Shalom and Xin Tian
ECE Department
University of Connecticut
Storrs, CT, USA
{tiy, ybs, xin.tian}@engr.uconn.edu

***Abstract*—Track-to-track fusion using estimates from multiple sensors can achieve better estimation performance than a single sensor. If the local sensors use different system models in different state spaces, the problem of heterogeneous track-to-track fusion arises. Compared with homogeneous track-to-track fusion that assumes the same system model for different sensors, the heterogeneous case poses two major challenges. First, the model heterogeneity problem, namely, that we have to fuse estimates from different state spaces (related by a certain nonlinear transformation); second, the estimation errors' dependence problem, which is generally recognized as the "common process noise effect". Different heterogeneous track-to-track fusion approaches, namely, the linear minimum mean square error approach and the maximum likelihood approach, are presented and compared with the corresponding centralized measurement tracker/fuser.**

***Index Terms*—heterogeneous track-to-track fusion, multisensor tracking, linear minimum mean square error, maximum likelihood fusion**

I. Introduction

In a multisensor tracking system the optimal estimate of a target's state can be obtained by a centralized tracker/fuser (CTF), i.e., directly sending to the fusion center (FC) all the measurements of the local sensors. However, in many practical situations, because of communication constraints, each local sensor has its own information processing system and sends only tracks to the FC, which fuses appropriately tracks from different local sensors to achieve comparable estimation performance to that of the CTF [3].

For track-to-track fusion (T2TF) from homogeneous local sensors, which use the same target state space, the "common process noise effect", quantified by the crosscovariance matrix, and the hierarchical tracking with different configurations for the real world have been theoretically well-established [3]. However, there is no known way for the calculation of the crosscovariance matrix in the case of heterogeneous local sensors. The difficulty to evaluate the crosscovariance matrix in the heterogeneous case is that it requires to capture the "common" part of process noises from different state spaces to quantify the crosscorrelation.

In the literature there are few works dealing with the model heterogeneity. A heterogeneous T2TF fusion approach was presented in [6] to fuse the tracks from an active sensor and a passive sensor with different state vectors. However, the fusion was done by using the full Cartesian state estimates (from an active sensor) to update the smaller angular state estimates (from a passive sensor). An expression for the steady state crosscovariance matrix for dissimilar sensors (of the same state vector but with different measurement noise variances) employing α–β filters was derived in [8]. For the specified case, a condition to guarantee the crosscovariance matrix's positivity was presented, which does not always hold in the heterogeneous case.

The goal of this paper is to fuse the tracks from heterogeneous local sensors (an active and a passive one) with different state spaces to yield fused estimates in the full state space and evaluate the performance of the resulting heterogeneous T2TF. The fusion configuration considered is the one without memory at the FC and no feedback to the local sensors (T2TFwoMnf in the terminology of [9]).

In view of the fact that there is no known way to evaluate the crosscovariance of the estimation errors in the case of heterogeneous sensors, a Monte Carlo (MC) investigation of these errors' crosscorrelations is carried out.

The paper is organized as follows. Section II formulates the heterogenous T2TF problem. Two approaches, namely, the linear minimum mean square error (LMMSE) and maximum likelihood (ML) heterogeneous T2TF are presented in Section III. The crosscorrelation analysis by MC simulations is presented in Section IV. Section V evaluates the proposed approaches in a tracking scenario with an active sensor and a passive sensor. Section VI provides conclusions.

II. The Heterogenous Track-to-Track Fusion Problem

Without loss of generality, consider the following state-space models

$$\mathbf{x}^i(k+1) = f^i[\mathbf{x}^i(k)] + \mathbf{v}^i(k) \tag{1}$$

$$\mathbf{z}^i(k) = h^i[\mathbf{x}^i(k)] + \mathbf{w}^i(k) \tag{2}$$

at sensor i and

$$\mathbf{x}^j(k+1) = f^j[\mathbf{x}^j(k)] + \mathbf{v}^j(k) \tag{3}$$

$$\mathbf{z}^j(k) = h^j[\mathbf{x}^j(k)] + \mathbf{w}^j(k) \tag{4}$$

at sensor j. In the above, $f^s[\cdot]$ and $h^s[\cdot]$, $s = i, j$, are different and can be nonlinear; $\mathbf{v}^s(\cdot)$ and $\mathbf{w}^s(\cdot)$, $s = i, j$, are the process and measurement noises, respectively.

Further, note that $\mathbf{x}^i$ and $\mathbf{x}^j$ are in different state spaces. Let $\mathbf{x}^i$ be the larger dimension state (e.g., full Cartesian position

Proc. 14th International Conference on Information Fusion, Chicago, Illinois, USA, July 2011.

978-0-9824438-2-8/11/$26.00 ©2011 IEEE

and velocity in 2-dimensional space for tracking with an active sensor)

$$\mathbf{x}^i = [\ x \quad \dot{x} \quad y \quad \dot{y}\ ]' \tag{5}$$

and $\mathbf{x}^j$ be the smaller dimension state (e.g., angular position and velocity for tracking with a passive sensor)

$$\mathbf{x}^j = [\ \theta \quad \dot{\theta}\ ]' \tag{6}$$

These state vectors have the nonlinear relationship

$$\mathbf{x}^j \triangleq g(\mathbf{x}^i) \tag{7}$$

The two sensors are assumed synchronized[1] and the time index k for sampling time t_k will be omitted if there is no ambiguity.

The corresponding estimates at these heterogeneous local sensors are $\hat{\mathbf{x}}^i$ with covariance matrix

$$P^i = E[(\mathbf{x}^i - \hat{\mathbf{x}}^i)(\mathbf{x}^i - \hat{\mathbf{x}}^i)'] \tag{8}$$

and $\hat{\mathbf{x}}^j$ with covariance matrix

$$P^j = E[(\mathbf{x}^j - \hat{\mathbf{x}}^j)(\mathbf{x}^j - \hat{\mathbf{x}}^j)'] \tag{9}$$

The problem is how to carry out the fusion of the estimate $\hat{\mathbf{x}}^i$ with P^i and the estimate $\hat{\mathbf{x}}^j$ with P^j to achieve a better estimation performance for the full state of interest $\mathbf{x}^i$.

III. The Heterogenous Track-to-Track Fusion

To illustrate the effect of the crosscovariance, consider the simple homogeneous T2TF in the linear-Gaussian and symmetric case with the local track covariance matrices $P_S^1 = P_S^2 = P_S$ and the crosscovariance matrices $P_S^{12} = P_S^{21} = P_S^X$. The resulting fused estimate and its covariance matrix are [3]

$$\begin{aligned} \hat{\mathbf{x}}_S^F &= \frac{1}{2}(\hat{\mathbf{x}}_S^1 + \hat{\mathbf{x}}_S^2) && (10)\\ P_S^F &= P_S^1 - (P_S^2 - P_S^{12}) \\ &\quad \cdot(P_S^1 + P_S^2 - P_S^{12} - P_S^{21})^{-1}(P_S^1 - P_S^{21}) \\ &= \frac{1}{2}P_S + \frac{1}{2}P_S^X && (11) \end{aligned}$$

In this case the fused estimate $\hat{\mathbf{x}}_S^F$ in (10) is independent of the crosscovariance because of the assumed symmetry. However, the corresponding covariance P_S^F in (11) has a term that depends on the crosscovariance. If $P_S^X > 0$, the fusion is optimistic if one ignores the crosscovariance (in which case the fuser calculated covariance is $\frac{1}{2}P_S$, i.e., smaller than what it should be); if $P_S^X < 0$, the fusion is pessimistic.

The crosscovariance for homogeneous fusion follows from a Lyapunov equation [3] and, consequently, it is always positive semi-definite. In the heterogeneous case while there is no known way to compute the crosscovariance matrix, shown in Appendix A using MC simulations, some of the crosscorrelations are positive and some are negative. They depend on the relative geometry of the two sensors and the target, as well as the target maneuvers. To further complicate the situation, the maneuvers are unknown deterministic, rather than (zero-mean white) process noise and the crosscovariance based on the process noise can be substantially different from what the maneuver causes.

The following subsections present two fusers that assume the crosscovariance is available.

A. The LMMSE Fuser

The first approach to heterogeneous T2TF is to use the linear technique based on the fundamental equations of LMMSE estimation [2]. Considering the full state estimate $\hat{\mathbf{x}}^i$ as the prediction and the smaller state estimate $\hat{\mathbf{x}}^j$ as the measurement, we have the LMMSE fused estimate

$$\hat{\mathbf{x}}^i_{\text{LMMSE}} = \hat{\mathbf{x}}^i + P^X(P^Z)^{-1}\left[\hat{\mathbf{x}}^j - g\left(\hat{\mathbf{x}}^i\right)\right] \tag{12}$$

with the corresponding fused covariance matrix

$$P^i_{\text{LMMSE}} = P^i - P^X(P^Z)^{-1}P^X \triangleq P^F \tag{13}$$

where

$$\begin{aligned} P^X &\triangleq E\left[\left(\mathbf{x}^i - \hat{\mathbf{x}}^i\right)\left(\hat{\mathbf{x}}^j - g(\hat{\mathbf{x}}^i)\right)'\right] \\ &\approx P^i(G^i)' - P^{ij} && (14)\\ P^Z &\triangleq E\left[\left(\hat{\mathbf{x}}^j - g(\hat{\mathbf{x}}^i)\right)\left(\hat{\mathbf{x}}^j - g(\hat{\mathbf{x}}^i)\right)'\right] \\ &\approx P^j - G^iP^{ij} - P^{ji}(G^i)' + G^iP^i(G^i)' && (15) \end{aligned}$$

where G^i is the Jacobian of $g(\mathbf{x}^i)$

$$G^i \triangleq \left[\nabla_{\mathbf{x}^i} g(\mathbf{x}^i)'\right]'|_{\mathbf{x}^i = \hat{\mathbf{x}}^i} \tag{16}$$

and P^{ij} is the crosscovariance matrix

$$P^{ij} \triangleq E[(\mathbf{x}^i - \hat{\mathbf{x}}^i)(\mathbf{x}^j - \hat{\mathbf{x}}^j)'] \tag{17}$$

B. The ML Fuser

Under the Gaussian assumption, the heterogeneous T2TF problem can be solved by minimumizing the negative log-likelihood function[2]

$$\begin{aligned} L &= -\ln p(\hat{\mathbf{x}}^i, \hat{\mathbf{x}}^j|\mathbf{x}^i) \\ &\propto \left(\begin{bmatrix} \hat{\mathbf{x}}^i \\ \hat{\mathbf{x}}^j \end{bmatrix} - \begin{bmatrix} \mathbf{x}^i \\ \mathbf{x}^j \end{bmatrix}\right)' P^{-1} \left(\begin{bmatrix} \hat{\mathbf{x}}^i \\ \hat{\mathbf{x}}^j \end{bmatrix} - \begin{bmatrix} \mathbf{x}^i \\ \mathbf{x}^j \end{bmatrix}\right) && (18) \end{aligned}$$

where (7) has been used and

$$P = \begin{bmatrix} P^i & P^{ij} \\ P^{ji} & P^j \end{bmatrix} \tag{19}$$

Then the ML fused estimate is the solution of

$$\nabla_{\mathbf{x}^i} L = 0 \tag{20}$$

Because of the nonlinearity of the function $g(\mathbf{x}^i)$, there is no explicit expression for the solution of (20). It can be solved by a numerical search, e.g., the gradient projection algorithm. The result is denoted as $\hat{\mathbf{x}}^i_{\text{ML}}$ and the corresponding covariance matrix is

$$P^i_{\text{ML}} = \left(\begin{bmatrix} I & G^i \end{bmatrix} P^{-1} \begin{bmatrix} I \\ G^i \end{bmatrix}\right)^{-1} \tag{21}$$

[1] Generalization to asynchronous sensors is possible [10], but the notations become very cumbersome.

[2] As it is pointed out in [4], the LMMSE T2TF approach is, in the linear Gaussian case, optimal in ML sense.

where G^i is defined in (16) and I is the identity matrix (4×4 in our case).

The results of $\hat{\mathbf{x}}^i_{\text{LMMSE}}$ with P^i_{LMMSE} and $\hat{\mathbf{x}}^i_{\text{ML}}$ with P^i_{ML} will be examined and compared with the CTF which processes all the measurements (from both the active and the passive sensor) in the FC in the simulation section.

IV. The Crosscorrelation in Heterogeneous Fusion

It has been recognized that, although different local sensors typically have independent measurement noises, the process noises for the motion models at these sensors belong to the same target and, consequently, will lead to (cross)correlated state estimation errors. This is the so-called "common process noise effect" [3]. For the heterogenous case, the common process noise effect, as it is embedded into the estimates from different sensors for the same target, also exists. However, since the estimates are in different state spaces, there is no known way to capture the "common" part exactly.

The dependence of the estimation errors can be quantified by the crosscovariance matrix, and the more accurately the crosscovariance matrix is obtained, the better the heterogeneous track-to-track fusion performance will be. However, the difference between the motion models for different sensors prohibits the evaluation of the crosscovariance matrix by the exact method described in [3] (limited to the homogeneous case and linear systems). Even this exact method is not considered practical since it requires information that is typically not available at the FC (the local filter gains).

While process noise is used in the motion equations to model the target maneuvers[3], these maneuvers are, however, not stochastic process. Consequently, MC simulations will be used to evaluate the crosscorrelation of the estimation errors from different sensors. As shown in Appendix A, considering the estimates from different local sensors in each MC run as one sample and evaluating the sample crosscorrelation coefficients, we observe both negative and positive crosscorrelations of the estimation errors from the heterogeneous local sensors in different parts of the target trajectory.

The fact that these crosscorrelations can be, unlike in the linear homogeneous case (when they are always positive), sometimes positive and sometimes negative is shown as follows. According to the (13), the information matrix (assuming we have P^{ij} and G is the Jacobian for conciseness) is

$$\begin{aligned} J &= (P^F)^{-1} \\ &\triangleq [P^i - [P^i(G^i)' - P^{ij}] \\ &\quad \cdot [P^j + G^i P^i (G^i)' + U]^{-1} [P^i(G^i)' - P^{ij}]']^{-1} \end{aligned} \tag{22}$$

where

$$U \triangleq -G^i P^{ij} - P^{ji}(G^i)' \tag{23}$$

Assuming $P^{ij} = 0$ (its elements are all zero), designated as the "uncorrelated" assumption (denoted concisely as "uncorr"), then (22) can be simplified (by the matrix inversion lemma) as

$$\begin{aligned} J(P^{ij}=0) &= \left[P^i - P^i(G^i)'[P^j + G^i P^i (G^i)']^{-1} G^i (P^i)'\right]^{-1} \\ &= (P^i)^{-1} - [(P^i)^{-1} P^i (G^i)'] \\ &\quad \cdot [G^i (P^i)' (P^i)^{-1} P^i (G^i)' - P^j - G^i P^i (G^i)']^{-1} [(P^i)^{-1} P^i (G^i)']' \\ &= (P^i)^{-1} + (G^i)' (P^j)^{-1} G^i \end{aligned} \tag{24}$$

If $P^{ij} \neq 0$ (this is denoted as "corr" for conciseness), then we have

$$\begin{aligned} J(P^{ij}\neq 0) &= (P^i)^{-1} - [(G^i)' - (P^i)^{-1} P^{ij}] \\ &\quad \cdot \left[[P^i(G^i)' - P^{ij}]' (P^i)^{-1} [P^i(G^i)' - P^{ij}] - [P^j + G^i P^i (G^i)' + U]\right]^{-1} \\ &\quad \cdot [(G^i)' - (P^i)^{-1} P^{ij}]' \\ &\triangleq (P^i)^{-1} + [(G^i)' - (P^i)^{-1} P^{ij}] [P^j + W]^{-1} [(G^i)' - (P^i)^{-1} P^{ij}]' \end{aligned} \tag{25}$$

where

$$\begin{aligned} W &\triangleq [G^i P^i (G^i)' + U] - [P^i(G^i)' - P^{ij}]' (P^i)^{-1} [P^i(G^i)' - P^{ij}] \\ &= -P^{ji} (P^i)^{-1} P^{ij} \end{aligned} \tag{26}$$

Equation (25) can be written as (the generic matrix inversion lemma is used)

$$\begin{aligned} J(P^{ij}\neq 0) &= (P^i)^{-1} + [(G^i)' - (P^i)^{-1} P^{ij}] \\ &\quad \cdot [(P^j)^{-1} - (P^j)^{-1} W (P^j)^{-1} [I + W(P^j)^{-1}]^{-1}] [(G^i)' - (P^i)^{-1} P^{ij}]' \\ &\triangleq (P^i)^{-1} + [(G^i)' - (P^i)^{-1} P^{ij}] [(P^j)^{-1} - K] [(G^i)' - (P^i)^{-1} P^{ij}]' \\ &\triangleq (P^i)^{-1} + (G^i)' (P^j)^{-1} G^i - K_c \\ &= J(P^{ij}=0) - K_c \end{aligned} \tag{27}$$

where I is the identity matrix and

$$K \triangleq (P^j)^{-1} W (P^j)^{-1} [I + W(P^j)^{-1}]^{-1} \tag{28}$$

$$\begin{aligned} K_c \triangleq\ & [(G^i)' - (P^i)^{-1} P^{ij}] K [(G^i)' - (P^i)^{-1} P^{ij}]' \\ & + (P^i)^{-1} P^{ij} (P^j)^{-1} G^i + [(P^i)^{-1} P^{ij} (P^j)^{-1} (G^i)]' \\ & - [(P^i)^{-1} P^{ij}] (P^j)^{-1} [(P^i)^{-1} P^{ij}]' \end{aligned} \tag{29}$$

Setting $P^{ij} = 0$ and $P^{ij} \neq 0$ for the estimation from the heterogenous local sensors correspond to "uncorr" and "corr" assumptions, respectively. For the homogeneous case, the crosscovariance matrix is always positive; this follows from the Lyapunov equation (9.3.2-3) in [3]. However, in the heterogeneous (and nonlinear) case, K_c may be indefinite (some eigenvalues are positive and some negative). Therefore, accounting for it (as opposed to assuming it zero) yields the exact (optimal) variance larger in some state components and smaller in others.

A procedure to account for the crosscovariance of the estimation errors ($\tilde{\mathbf{x}}^i$ and $\tilde{\mathbf{x}}^j$) by using a simple functional model of their crosscorrelations (based on the polar-to-Cartesian transformation) is described in [12]. However, this did not provide any perceivable benefits. Thus, since the maneuvers are unknown and scenario dependent, we pursue the heterogeneous T2TF without considering the crosscorrelation between the estimation errors.

[3]The whiteness is necessary so the state is a Markov process, a sine qua non prerequisite for any recursive estimation algorithm [2].

V. Simulation results

A typical 2-dimensional scenario for heterogenous T2TF is with an active sensor located at $(x_a,\ y_a)$, with measurements of target range and azimuth angle

$$r = \sqrt{(x-x_a)^2+(y-y_a)^2}+w_r \quad (30)$$

$$\theta_a = \tan^{-1}\left(\frac{y-y_a}{x-x_a}\right)+w_a \quad (31)$$

and a passive sensor located at $(x_p,\ y_p)$, with the azimuth angle measurements

$$\theta_p = \tan^{-1}\left(\frac{y-y_p}{x-x_p}\right)+w_p \quad (32)$$

where w_r, w_a and w_p are mutually independent zero mean Gaussian noises with standard deviations (SD) σ_r, σ_a and σ_p, respectively.

The ground truth is a target moving with a constant speed of 250 m/s with initial state in Cartesian coordinates (with position in m)

$$\mathbf{x}^i(0) = [\ x(0)\ \ \dot{x}(0)\ \ y(0)\ \ \dot{y}(0)\ ]' = [\ 0\ \ 0\ \ 20000\ \ 250\ ]' \quad (33)$$

At $t=100$ s it starts a left turn of 2°/s (about 30 mrad/s) for 30 s, then continues straight until $t=200$ s, at which time it turns right with 1°/s for 45 s, then left with 1°/s for 90 s, then right with 1°/s for 45 s, then continues straight until 50 s.

The measurements of the active sensor located at $(-6\cdot 10^4,\ 2\cdot 10^4)$ m are made every $T_a=5$ s and starting from $k=0$ with measurement noise $\sigma_r=20$ m and $\sigma_a=5$ mrad. The measurements of the passive sensor located at $(-5\cdot 10^4,\ 4\cdot 10^4)$ m are made every $T_p=1$ s and starting from $k=0$ with measurement noise $\sigma_p=0.5$ mrad. This scenario is shown in Fig.1.

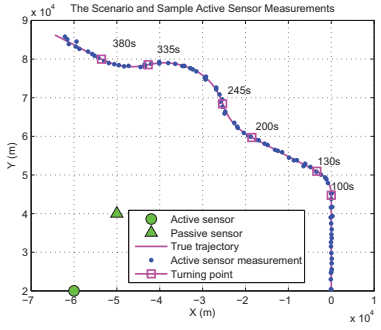

Figure 1: The scenario.

In order to cover the uniform motion segments and maneuvering segments in the trajectory, the active sensor uses an interacting multiple model (IMM, more precisely, the IMM with coordinated turn, i.e., IMM-CT) estimator, using continuous time white noise acceleration (CWNA) model [2], with two modes with different process noise levels. For reasons shown in Appendix B, a linear Kalman filter (KF), using a continuous time Wiener process acceleration (CWPA) model [2], is used for the passive sensor.

For the active sensor, we first use an unbiased measurement conversion from polar coordinates to Cartesian coordinates [2]. As assuming a nearly "coordinated turn" (CT) model, the state vector is augmented as (note that $\mathbf{x}^i$ is the state of interest for further heterogeneous T2TF)

$$\mathbf{x}_a^i(k) \triangleq [\ x(k)\ \ \dot{x}(k)\ \ y(k)\ \ \dot{y}(k)\ \ \Omega(k)\ ]' = [\ \mathbf{x}^i(k)'\ \ \Omega(k)\ ]' \quad (34)$$

The discretized CWNA model [2] with the augmented state vector is

$$\mathbf{x}_a^i(k+1) = F_a^i(k)\mathbf{x}_a^i(k)+\mathbf{v}_a^i(k) \quad (35)$$

$$\mathbf{z}_a^i(k) = h_a^i[\mathbf{x}_a^i(k)]+\mathbf{w}_a^i(k) \quad (36)$$

where, with T_a the sampling interval of the active sensor,

$$F_a^i(k)=\begin{bmatrix} 1 & \frac{\sin\Omega(k)T_a}{\Omega(k)} & 0 & -\frac{1-\cos\Omega(k)T_a}{\Omega(k)} & 0 \\ 0 & \cos\Omega(k)T_a & 0 & -\sin\Omega(k)T_a & 0 \\ 0 & \frac{\cos\Omega(k)T_a}{\Omega(k)} & 1 & \frac{\sin\Omega(k)T_a}{\Omega(k)} & 0 \\ 0 & \sin\Omega(k)T_a & 0 & \cos\Omega(k)T_a & 0 \\ 0 & 0 & 0 & 0 & 1 \end{bmatrix} \quad (37)$$

$$h_a^i[\cdot] = \tan^{-1}\frac{y(k)-y_a(k)}{x(k)-x_a(k)} \quad (38)$$

and the the covariance matrix of the process noise is

$$Q_a^i(k) \triangleq E\left[\mathbf{v}_a^i(k)\mathbf{v}_a^i(k)'\right] = \begin{bmatrix} \begin{bmatrix} \frac{T_a^3}{3} & \frac{T_a^2}{2} \\ \frac{T_a^2}{2} & T_a \end{bmatrix} q_a & \mathbf{0}_{2\times 2} & 0 \\ \mathbf{0}_{2\times 2} & \begin{bmatrix} \frac{T_a^3}{3} & \frac{T_a^2}{2} \\ \frac{T_a^2}{2} & T_a \end{bmatrix} q_a & 0 \\ 0 & 0 & T_a q_\Omega \end{bmatrix} \quad (39)$$

where the continuous time process noise "intensities" q_a and q_Ω are the power spectral densities (PSD). Note that the process noise induced root mean square (RMS) change rate in the velocity and in the turn rate over a sampling interval T_a are

$$d_a \triangleq \frac{\sqrt{q_a T_a}}{T_a} \qquad d_\Omega \triangleq \frac{\sqrt{q_\Omega T_a}}{T_a} \quad (40)$$

whose physical dimensions are linear and turn acceleration [11]. These are the design values used to select the process noise PSD.

As the CT model described in (35) is nonlinear, EKF has been used as the mode-matched filter for IMM-CT (the detailed EKF equations can be found in [2]). We only use the estimate $\hat{\mathbf{x}}^i(k)$ (from $\hat{\mathbf{x}}_a^i(k)$) and the corresponding covariance matrix $P^i(k)$ for the fusion.

For the active sensor IMM-CT, the process noises design values are summarized in Table I.

Table I: The RMS change rate due to process noise

	d_a [(m/s)/s]	d_Ω [(mrad/s)/s]
Mode 1	0.03	0.05
Mode 2	4	0.5

The transition probability matrix of the IMM-CT estimator used at the active sensor is (based on the mean sojourn time

[2])

$$\pi_{CT} = \begin{bmatrix} 0.8 & 0.2 \\ 0.2 & 0.8 \end{bmatrix} \tag{41}$$

with initial mode probability vector $[\,0.7,\ \ 0.3\,]$.

As pointed out in Appendix C, the target maneuvering index for the passive sensor is very small. Consequently, a single model filter (i.e., a KF) has been chosen as the local estimator for the passive sensor, with the state vector

$$\mathbf{x}_p^j \triangleq [\ \theta \quad \dot{\theta} \quad \ddot{\theta}\ ]' = [\ \mathbf{x}^j(k)' \quad \ddot{\theta}\ ]' \tag{42}$$

the (discretized) CWPA model [2] in the angle, angle rate and angle acceleration space is

$$\mathbf{x}_p^j(k+1) = F_p^j \mathbf{x}_p^j(k) + \mathbf{v}_p^j(k) \tag{43}$$

$$\mathbf{z}_p^j(k) = H_p^j \mathbf{x}_p^j(k) + \mathbf{w}_p^j(k) \tag{44}$$

where, with T_p the sampling interval of the passive sensor,

$$F_p^j = \begin{bmatrix} 1 & T_p & \frac{T_p^2}{2} \\ 0 & 1 & T_p \\ 0 & 0 & 1 \end{bmatrix} \tag{45}$$

$$H_p^j = [\ 1 \quad 0 \quad 0\ ]' \tag{46}$$

and the covariance matrix of the process noise is

$$\begin{aligned} Q_p^i(k) &\triangleq E\left[\mathbf{v}_p^j(k)\mathbf{v}_p^j(k)'\right] \\ &= \begin{bmatrix} \frac{T_p^5}{20} & \frac{T_p^4}{8} & \frac{T_p^3}{6} \\ \frac{T_p^4}{8} & \frac{T_p^3}{3} & \frac{T_p^2}{2} \\ \frac{T_p^3}{6} & \frac{T_p^2}{2} & T_p \end{bmatrix} q_p \end{aligned} \tag{47}$$

Note that for the PSD q_p, the process noise induced RMS change in the angular acceleration over T_p is

$$d_p \triangleq \frac{\sqrt{q_p T_p}}{T_p} \tag{48}$$

whose physical dimension is angular jerk (derivative of acceleration).

The process noise design value chosen for the passive sensor is $d_p = 0.04$ [(mrad/s^2)/s]. We only use the estimate $\hat{\mathbf{x}}^j(k)$ (from $\hat{\mathbf{x}}_p^j(k)$) and the corresponding covariance matrix $P^j(k)$ for the fusion.

The LMMSE and ML heterogeneous T2TF are carried out at the FC every $T_f = 5$ s under the "uncorr" assumption, with the local estimates $\hat{\mathbf{x}}^i(k)$ (from $\hat{\mathbf{x}}_a^i(k)$) and $\hat{\mathbf{x}}^j(k)$ (from $\hat{\mathbf{x}}_p^j(k)$) and their corresponding covariance matrices $P^i(k)$ and $P^j(k)$. The CTF uses the same IMM design (CTF IMM for short) as the active sensor IMM and uses parallel updating technique when both active and passive measurements are received at the same time [3]. The FC can run the fusion at an arbitrarily low rate or "on demand".

A. The LMMSE Fuser

In Figs. 2 and 3, the root mean square errors (RMSE) for the LMMSE fuser (with $T_f = 5$ s under the "uncorr" assumption) are compared with those for the active sensor's IMM estimator and the CTF IMM in position and velocity, respectively. It can be seen that the LMMSE heterogeneous T2TF approach always provides significantly better estimation performance than the single (active) sensor case.

The LMMSE heterogeneous T2TF provides larger RMSE than the CTF IMM in the non-maneuvering intervals but smaller RMSE if there is a maneuver. This degradation of the CTF in both position and velocity during the maneuvering intervals is because the CTF is using an IMM estimator, which is inappropriate for the passive sensor (due to the very small maneuver index). While using the IMM estimator is generally beneficial for maneuvering targets, the use of an IMM estimator with a sensor that cannot "see" the maneuvers can lead to performance degradation (the CTF IMM's performance at some fusion points is even worse than the active sensor IMM's). As shown in Appendix B, the maneuvering index from the passive sensor's view is so small that when the passive sensor measurements (with higher sampling rate than those of the active sensor) are sent to FC and processed centrally, these measurements increase the uncertainty about the target maneuvers.

The observation from Figs. 2 and 3 that CTF IMM performs during target maneuvers worse than the heterogeneous T2TF points out that the heterogeneous T2TF benefits from the freedom of having more suitable filters for the individual local sensors. This freedom can provide final fusion results comparable or even better than the corresponding CTF estimator.

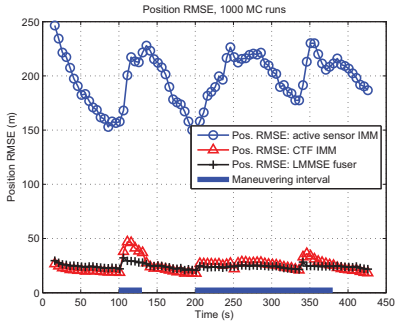

Figure 2: The position RMSE for LMMSE fuser.

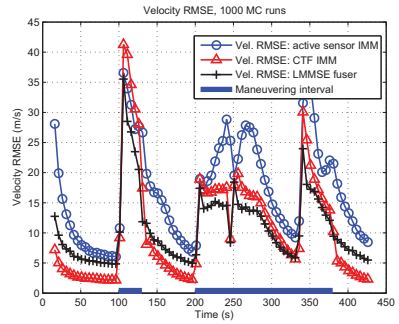

Figure 3: The velocity RMSE for LMMSE fuser.

We evaluate the fusion consistency of the LMMSE fuser by the normalized estimation error square (NEES) consistency test [2]. The NEES for the LMMSE fusion approach are

shown in Fig. 4. The reason for the inconsistency of the fused estimates are (i) the local IMM estimator (for the active sensor) and the KF estimator (for the passive sensor) are not entirely consistent[4] (as shown in Appendix C) and (ii) the crosscovariance has been assumed zero. Nevertheless, the quality of the estimates is improved by fusion, which justifies the approach. At this point, there is no known way to improve the sometimes optimistic, sometimes pessimistic behavior of the IMM — it is the inconsistency that drives its adaptation.

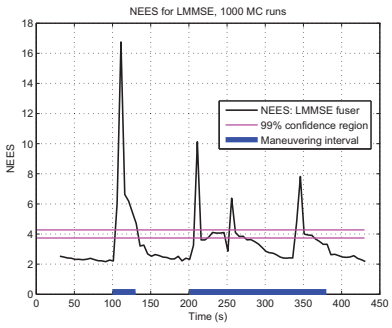

Figure 4: The NEES for LMMSE fuser.

B. The ML Fuser

Using a numerical search (the gradient projection algorithm), the RMSE in position and velocity for the ML fuser are shown (with $T_f = 5$ s under the "uncorr" assumption) in Fig. 5 and Fig. 6, respectively. It can be seen that both the LMMSE fuser and the ML fuser give nearly the same RMSE in position and velocity and both have better performances than the single (active) sensor case. As pointed out in [4], the LMMSE fuser is, in the linear-Gaussian case, actually optimal in the ML sense. Since the ML fuser in the heterogenous case (with nonlinearity) needs to be implemented by a time-consuming numerical search, the LMMSE fuser can be considered as an efficient and effective alternative for the ML fuser.

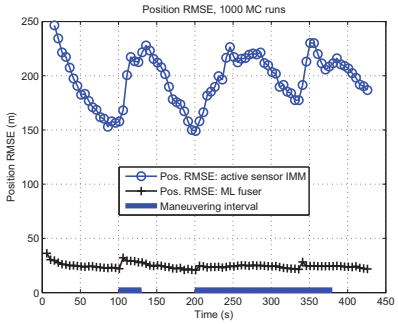

Figure 5: The position RMSE for ML fuser.

[4]The IMM estimator is the worst estimator in terms of consistency except for all the other estimators [3]. However, it is the "short term" inconsistency that is the key for the capability of the IMM estimator to adapt itself to the observed behavior of the target (large innovations).

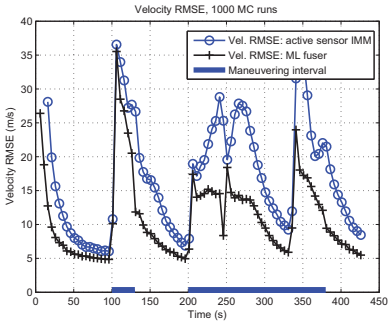

Figure 6: The velocity RMSE for ML fuser.

VI. Conclusions

Examining the differences between the heterogeneous and homogeneous T2TF, this paper investigates the major difficulties of heterogenous T2TF. The LMMSE and the ML approaches for heterogenous T2TF are presented and compared with the corresponding CTF. The simulation study shows that both approaches can effectively achieve improved performance over the single sensor track quality and comparable performance to the CTF track. The use of IMM estimator when there is no need for it (to process the measurements from the passive sensor in the case considered) can lead to performance degradation of the CTF. On the other hand, the freedom available to each local sensor to flexibly design a more suitable local estimator allows the heterogeneous T2TF approach to achieve a better estimation performance. As the LMMSE T2TF has practically the same performance as the ML T2TF, it can be considered as an effective and efficient alternative for the numerical search required by the ML approach. The estimation errors' crosscorrelation has been examined by MC simulations. As it is impossible to predict maneuvers in a trajectory and there is no known way to correctly quantify the crosscorrelation of the estimation errors from heterogeneous local sensors, the heterogeneous T2TF was carried out assuming the tracks from the heterogeneous local sensors as uncorrelated.

Appendix A
The MC Results for the Sample Crosscorrelation

The *sample crosscorrelation coefficient* between the lth component of $\mathbf{x}^i$ and the hth component of $\mathbf{x}^j$ in M MC runs at a particular point in time (not indicated, for conciseness) is

$$\hat{\rho}^M_{\mathbf{x}^i_l \mathbf{x}^j_h} \triangleq \frac{\sum_{m=1}^{M} (\hat{\mathbf{x}}^i_{l,m} - \mathbf{x}^i_l)(\hat{\mathbf{x}}^j_{h,m} - \mathbf{x}^i_h)}{\sqrt{\left[\sum_{m=1}^{M} (\hat{\mathbf{x}}^i_{l,m} - \mathbf{x}^i_l)^2\right] \left[\sum_{m=1}^{M} (\hat{\mathbf{x}}^j_{h,m} - \mathbf{x}^j_h)^2\right]}} \quad (49)$$

The sample crosscorrelation coefficients of different heterogeneous components from 1000 MC runs, for the scenario described in Section V, are shown in Figs. 7–10. It can be seen that the "common process noise effect", driven by real maneuvers here, leads to significant crosscorrelation between the estimation errors from the heterogeneous local sensors. Furthermore, both positive and negative crosscorrelation

are observed. This motivates the geometry-based "functional model" discussed in [12].

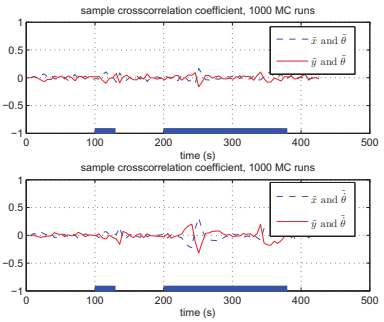

Figure 7: The sample crosscorrelation analysis for $\tilde{x}$ and $\tilde{y}$ with $\tilde{\theta}$ and $\dot{\tilde{\theta}}$.

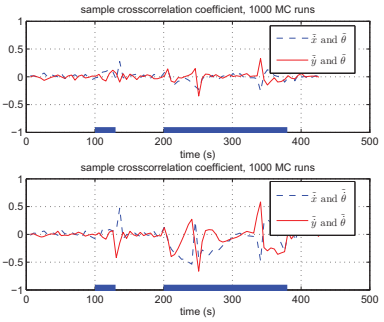

Figure 8: The sample crosscorrelation analysis for $\tilde{\tilde{x}}$ and $\tilde{\tilde{y}}$ with $\tilde{\theta}$ and $\dot{\tilde{\theta}}$.

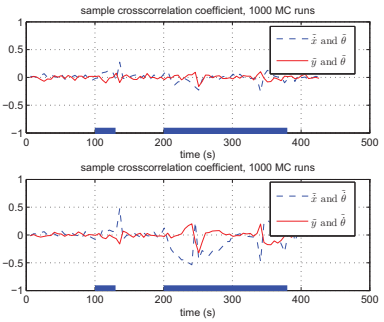

Figure 9: The sample crosscorrelation analysis for $\tilde{\tilde{x}}$ and $\tilde{y}$ with $\tilde{\theta}$ and $\dot{\tilde{\theta}}$.

Appendix B
The Choice of Estimator for the Passive Sensor

The guideline for deciding whether to use an IMM estimator or a (single model) KF can be quantified in terms of the target maneuvering index, which is the ratio between the standard deviation (RMS values) of the motion uncertainty and the

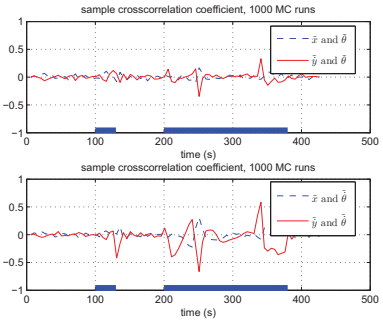

Figure 10: The sample crosscorrelation analysis for $\tilde{x}$ and $\tilde{\tilde{y}}$ with $\tilde{\theta}$ and $\dot{\tilde{\theta}}$.

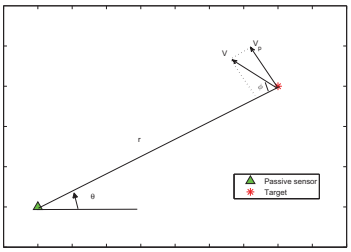

Figure 11: The illustrated scenario for calculating target maneuvering index.

measurement uncertainty [2] [7]. Namely, if this index is below 0.5 then there is no point in using an IMM.

For the passive sensor considered, the maneuvering index can be calculated as follows. As shown in Fig. 11, the angular velocity seen by the passive sensor is

$$\dot{\theta}_p = \frac{V \sin\varphi}{r_p} \tag{50}$$

where V is the speed of the target and r_p is the range of the target from the passive sensor. Then the angular acceleration seen by the passive sensor is

$$\ddot{\theta}_p = \frac{V \cos\varphi}{r_p}\dot{\varphi} \tag{51}$$

where $\dot{\varphi}$ is the target turn rate.

The RMS effect of (51) on the (angular) position, i.e., the angular displacement over sampling interval T_p (multiplied by 2) is $\ddot{\theta}_p T_p^2$. The (target's true) maneuvering index, with the passive sensor noise SD σ_p (in radians), is the (physically dimensionless) quantity

$$\lambda_p \quad = \quad \frac{\ddot{\theta}_p T_p^2}{\sigma_p} = \frac{\dot{\varphi} T_p^2 V \cos\varphi}{\sigma_p r_p} \tag{52}$$

For the scenario described in the simulation section, with $V = 250\,\text{m/s}$, $\cos\varphi \approx 0.8$, $r_p \approx 5 \cdot 10^4\,\text{m}$, $T_p = 1\,\text{s}$, $\sigma_p = 0.5\,\text{mrad}$ and $\dot{\varphi} \approx 30\,\text{mrad/s}$ (which is the maximum target turn rate in our simulation scenario), we have $\lambda_p \approx 0.24$. This small target maneuvering index (less than 0.5) leads to the choice of a KF for the passive sensor, as done in Section V.

APPENDIX C
THE LOCAL ESTIMATOR'S CONSISTENCY

The NEES for the active sensor's IMM and for the passive sensor's KF are shown in Figs. 12 and 13, respectively. The lack of consistency of the passive sensor KF is due to the maneuvers. The lack of consistency of the active sensor IMM is common and this is due to its (unavoidable delay) in the adaptation. The IMM is "pessimistic" during the no-maneuver intervals and "optimistic" when a maneuver starts or ends until it "catches up". This is the typical behavior of the IMM, which is still superior to any single-model based filter.

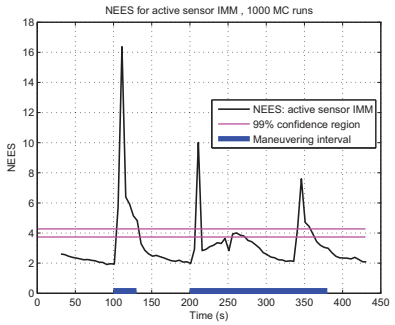

Figure 12: The NEES for active sensor IMM.

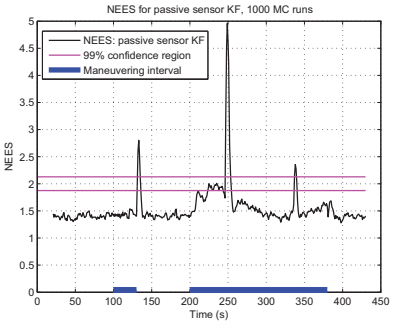

Figure 13: The NEES for passive sensor KF.

REFERENCES

[1] Y. Bar-Shalom and H. Chen, "Covariance Reconstruction for Track Fusion with Legacy Track Sources", *J. of Advances in Information Fusion*, 3(2):107–117, Dec. 2008.

[2] Y. Bar-Shalom, X.R. Li, and T. Kirubarajan, *Estimation with Applications to Tracking and Navigation: Algorithms and Software for Information Extraction*, Wiley, 2001.

[3] Y. Bar-Shalom, P.K. Willett and X. Tian, *Tracking and Data Fusion*, YBS Publishing, 2011.

[4] K.C. Chang, R.K. Saha and Y. Bar-Shalom, "On Optimal Track-to-Track Fusion", *IEEE Trans. Aerosp. Electronic Systems*, 33(4):1271–1276, Oct. 1997.

[5] H. Chen, T. Kirubarajan, and Y. Bar-Shalom, "Performance Limits of Track-to-Track Fusion versus Centralized Estimation: Theory and Application", *IEEE Trans. Aerosp. Electronic Systems*, AES-39(2):386–398, Apr. 2003.

[6] H. Chen and Y. Bar-Shalom, "Track Association and Fusion with Heterogeneous Local Trackers", *Proc. 46th IEEE Conf. on Decision and Control*, New Orleans, LA, Dec. 2007.

[7] T. Kirubarajan and Y. Bar-Shalom, "Kalman filter versus IMM estimator: when do we need the latter?", *IEEE Trans. Aerosp. Electronic Systems*, 39(4):1452–1457, Oct. 2003.

[8] R.K. Saha "Track-to-Track Fusion With Dissimilar Sensors", *IEEE Trans. Aerosp. Electronic Systems*, 32(3):1021–1029, July 1996.

[9] X. Tian and Y. Bar-Shalom, "Track-to-Track Fusion Configurations and Association in a Sliding Window", *J. of Advances in Information Fusion*, 4(2):146-164, Dec. 2009.

[10] X. Tian and Y. Bar-Shalom, "The Optimal Algorithm for Asynchronous Track-to-Track Fusion", *Proc. SPIE Conf. Signal and Data Processing of Small Targets*, #7698-46, Orlando, FL, April 2010.

[11] T. Yuan, Y. Bar-Shalom, P.K. Willett and D. Hardiman, "Impact Point Prediction for Short Range Thrusting Projectiles", *Proc. SPIE conference Signal and Data Processing of Small Targets*, #7698-55, Orlando, FL, April 2010.

[12] T. Yuan, Y. Bar-Shalom and X. Tian, "Heterogeneous Track-to-Track Fusion", *J. of Advances in Information Fusion*, submitted for publication, 2011.